DOI: 10.1002/cmdc.201000191

Synthesis and Evaluation of Bombesin Analogues Conjugated to Two Different Triazolyl-Derived Chelators for ^{99m}Tc Labeling

Luc Brans,[a] Elisa García-Garayoa,[b] Christian Schweinsberg,[b] Veronique Maes,[a] Harriet Struthers,[c] Roger Schibli,[b, c] and Dirk Tourwé*[a]

Overexpression of the gastrin-releasing peptide receptor (GRPR) in a variety of human carcinomas has provided a means of diagnosis and treatment. Previously we reported a metabolically stable (N^{α}His)Ac-βAla-βAla-[Cha^{13},Nle^{14}]BBS(7–14) analogue with high affinity for the GRPR. We have also shown that the biodistribution pattern of this fairly lipophilic, radiolabeled peptide can be enhanced by glycation, which is easily carried out by Cu^{I}-catalyzed cycloaddition. Herein, we further elaborate this "click approach" in the synthesis of a new series of triazole-based chelating systems as alternatives to the (N^{α}His)Ac chelator for labeling with the ^{99m}Tc(CO)$_3$ core. The bombesin analogues, containing these new chelating systems, were evaluated with regard to their synthesis and in vitro and in vivo properties, and were compared with their (N^{α}His)Ac counterparts. The influence of the chelator on biodistribution properties was less than that of glycation, which clearly improved the tumor-to-background ratios.

Introduction

Bombesin (BBS) is a 14 amino acid peptide (pGlu^1-Gln^2-Arg^3-Leu^4-Gly^5-Asn^6-Gln^7-Trp^8-Ala^9-Val^{10}-Gly^{11}-His^{12}-Leu^{13}-Met^{14}-NH$_2$) that was isolated from the frog *Bombina bombina* by Anastasi et al.[1] Since then, two bombesin-like peptides have been found in mammals: gastrin-releasing peptide (GRP)[2] and neuromedin B (NMB).[3] These peptides contain 27 and 10 amino acids, respectively, and have high homology with BBS. In mammals, three BBS receptor subtypes have been characterized to date which all belong to the family of G-protein-coupled receptors.[4] The NMBR, or BB$_1$ receptor, subtype has high affinity for NMB. The GRPR, or BB$_2$ receptor, has high affinity for GRP and an even higher affinity for BBS. The third subtype, BB$_3$, is an orphan receptor, as no high-affinity endogenous ligand has been identified yet. The C-terminal nonapeptide sequence, BBS(6–14), is the minimal fragment necessary to maintain full GRPR affinity. Heimbrook et al. determined that acetylation of the N-terminal amine in the octapeptide sequence Ac-BBS(7–14) maintained affinity at nanomolar levels.[5,6]

In addition to the presence of BBS receptors in the periphery and the central nervous system, evidence has been found that these receptors are overexpressed on the membrane of several tumor cells,[7] including prostate, breast, colon, and small-cell lung carcinomas.[8–14] This provides an opportunity to use the GRPR as a target for detection and treatment[15] of these cancers using radiolabeled BBS(7–14) ligands. Several ^{18}F, ^{64}Cu, ^{68}Ga, ^{99m}Tc, ^{177}Lu, ^{111}In, and ^{188}Re radiolabeled BBS(7–14) derivatives have already been designed as tumor-selective tracers for peptide receptor imaging and radiotherapy, but most of them suffer from high uptake in the abdomen.[7,16–20] This is also the case for the ^{99m}Tc(CO)$_3$-labeled (N^{α}His)Ac-βAla-βAla-[Cha^{13},Nle^{14}]BBS(7–14) (**1**; Figure 1) which we previously reported.[21]

To be useful for the diagnosis of abdominal lesions, a radiotracer must accumulate at the lowest possible levels in the abdomen, including in the liver and the intestines. Uptake at these organs depends mainly on pharmacokinetic properties, which are influenced by factors such as metabolic stability,[21] polarity,[22,23] and charge.[24–26] Therefore, we evaluated different glycation techniques for (N^{α}His)Ac-containing bombesin analogues.[27] Bombesin analogue **2**, which was glycated by Cu^{I}-catalyzed alkyne/azide cycloaddition, exhibited an improved biodistribution profile in PC-3 xenografts, resulting in nude mice with enhanced tumor uptake, decreased hepatic activity, and expedient excretion by the kidneys.[28] Glycation by Cu^{I}-catalyzed cycloaddition also prevented glycation of the secondary amine in the (N^{α}His)Ac chelator, which was encountered during Maillard glycation.[27,29]

An alternative to the N^{α}-carboxymethylhistidine [(N^{α}His)Ac] chelator for ^{99m}Tc(CO)$_3$, which requires multistep synthesis, is a 1,2,3-triazole-containing chelator. We recently reported the single step synthesis of such a 1,2,3-triazole-containing chelator by alkyne/azide cycloaddition.[30,31] Preliminary data regard-

[a] Dr. L. Brans, Dr. V. Maes, Prof. D. Tourwé
Department of Organic Chemistry
Vrije Universiteit Brussel, 1050 Brussels (Belgium)
Fax: (+32) 02-629-33-04
E-mail: datourwe@vub.ac.be

[b] Dr. E. García-Garayoa, Dr. C. Schweinsberg, Prof. R. Schibli
Center for Radiopharmaceutical Science
Paul Scherrer Institute, 5232 Villigen-PSI (Switzerland)

[c] Dr. H. Struthers, Prof. R. Schibli
Department of Chemistry and Applied Biosciences
ETH Zurich, 8093 Zurich (Switzerland)

Supporting information for this article is available on the WWW under http://dx.doi.org/10.1002/cmdc.201000191.

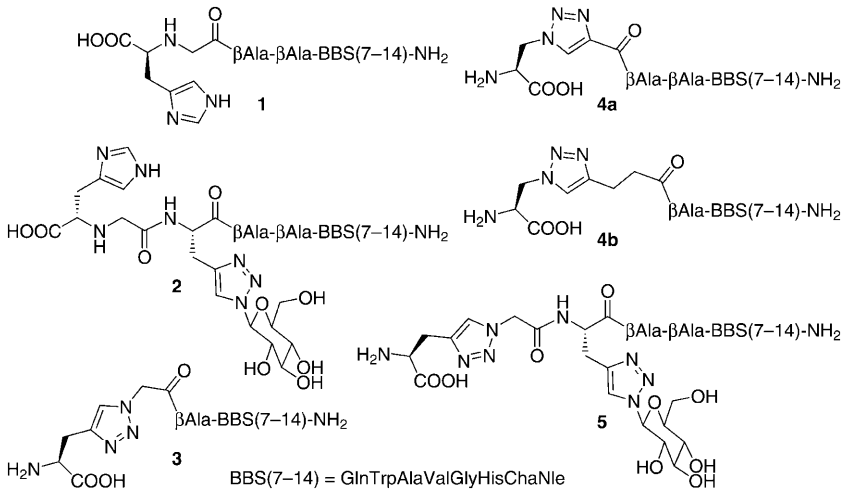

Figure 1. Overview of the bombesin analogues.

ing $^{99m}Tc(CO)_3$-labeled bombesin analogue **3** have been previously reported.[30]

We report herein the detailed synthesis of bombesin analogues conjugated to two types of triazole-based chelators for labeling with the readily available $^{99m}Tc(CO)_3$ core. These triazole-based chelators (**3**, **4a/b**, and **5**) do not contain the reactive secondary amine, thus permitting selective derivatization of the peptide sequence, which can be carried out after chelator conjugation. This is in contrast to peptides containing the (N^{α}His)Ac chelator (**1** and **2**) in which selective glycation by Maillard reaction was hampered by the secondary amine of the (N^{α}His)Ac chelator.[29] The labeling and in vitro and in vivo properties of analogues **3**–**5**, (Figure 1) are compared with (N^{α}His)Ac-containing counterparts **1** and **2**. Therefore, the previously published data for **1** and **2** is presented for comparison.

Results and Discussion

Synthesis

The discovery by Tornøe[32] that the slow cycloaddition of an azide and an alkyne can be accelerated by Cu^{I} catalysis, which was primarily developed further by the Sharpless group,[33,34] led to addition of an important new member to the family of "click" reactions. In fact, the popularity of this reaction and the constant use of the term "click" in this regard has led to the common misuse of "click" to denote only the Cu^{I}-catalyzed reaction between an azide and an alkyne.

We applied the click reaction of an azide and an alkyne to synthesize two chelators as alternatives for the histidine-like chelators (N^{α}His)Ac and (N^{ε}His)Ac, which were previously developed by our research group and by Alberto et al., respectively.[35,36] The resulting triazole ring is known to be a good ligand for various transition metals.[37] We evaluated the synthesis of these triazole-based chelators and their capacity for labeling with the $^{99m}Tc(CO)_3$ core. The biodistribution of these triazole-containing bombesin analogues was compared with the corresponding (N^{α}His)Ac analogues.

Two varieties of triazole-based chelators were constructed on a resin-bound bombesin sequence. The first type, seen in **8** (Scheme 1), is obtained by "clicking" the commercially available Boc-propargylglycine (Boc-Pra-OH; **7**) to the azidoacetylated peptide (**6**).[30] The cycloaddition reaction went to completion upon shaking the solid-supported azidopeptide (**6**; 1.0 equiv) overnight with Boc-Pra-OH (**7**; 2.0 equiv), *N*,*N*-diisopropylethylamine (DIEA; 2.0 equiv), and CuI (0.2 equiv) in *N*,*N*-dimethylformamide (DMF). Cleavage of bound peptide **8** from the resin with simultaneous side chain deprotection afforded bombesin analogue **3**. The resulting chelator, β-(1-peptidyl-1*H*-[1,2,3]triazol-4-yl)Ala, is denoted as β1TA, where the number 1 indicates the position to which the peptide chain is attached. This nomenclature is unambiguous, considering the 1,4-regiospecificity of Cu^{I}-catalyzed alkyne/azide cycloaddition.

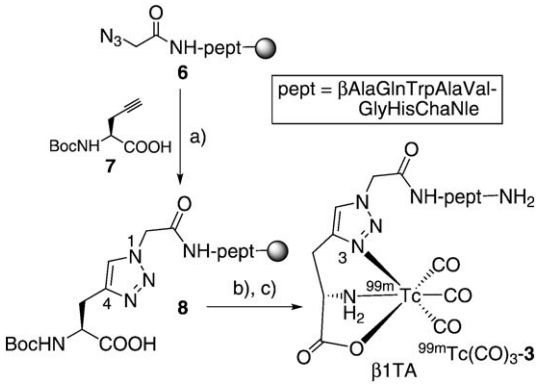

Scheme 1. Synthesis and radiolabeling of β1TA-containing bombesin analogues. a) **7** (2.0 equiv), CuI (0.2 equiv), DIEA (2.0 equiv), DMF, 16 h; b) 10% TA/EDT (7:3) in TFA, 3 h; c) $[^{99m}Tc(CO)_3(H_2O)_3]^+$.

The [Cha^{13},Nle^{14}]BBS(7–14) sequence was used for all analogues.[38] Both substitutions stabilized the binding sequence while retaining binding affinity. Either one or two βAla residues were used as a spacer between the chelator and the binding sequence to minimize the influence of the bulky radiometal complex on binding affinity for the GRPR. It was also shown that the $(\beta Ala)_2$ spacer in (N^{α}His)Ac-βAla-βAla-[Cha^{13},Nle^{14}]BBS-(7–14) (**1**) improved the biodistribution profile by improving in vivo tumor uptake.[21]

The second type of triazole chelator is obtained by Cu^{I}-catalyzed alkyne/azide cycloaddition of Boc-βN_3Ala-OH (**16**) and an alkynoic acid (**10** or **11**), coupled to the resin-supported peptide **9** (Scheme 2). This provides the β-(4-peptidyl-1*H*-[1,2,3]tria-

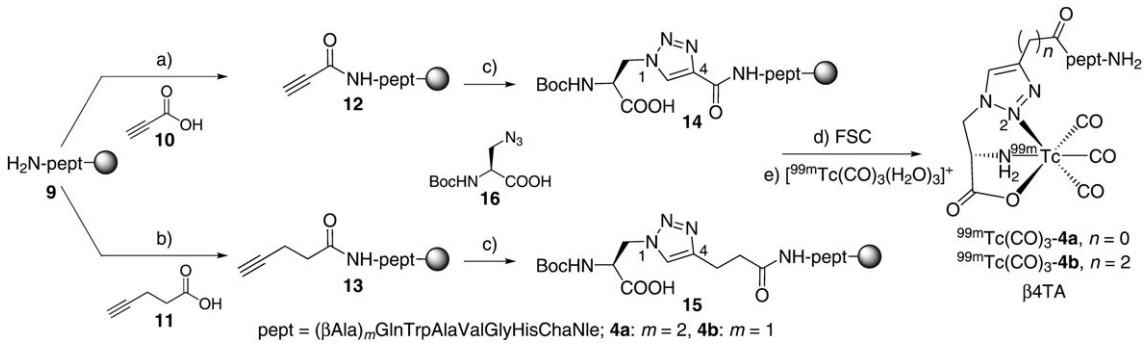

Scheme 2. Synthesis and radiolabeling of β4TA-containing bombesin analogues. a) **10** (3.0 equiv), DIC (3.0 equiv), HOBt (3.0 equiv), DMF, 2 h; b) **11** (3.0 equiv), DIC (3.0 equiv), HOBt (3.0 equiv), DMF, 2 h; c) **16** (2.0 equiv), CuI (0.2 equiv), DIEA (2.0 equiv), DMF, 16 h; d) 10% TA/EDT (7:3) in TFA, 3 h; e) $[^{99m}Tc(CO)_3(H_2O)_3]^+$.

zol-1-yl)Ala chelator (**4a/b**), abbreviated as β4TA, due to the attachment of the peptide chain to position four of the five-membered ring. Boc-βN_3Ala-OH (**16**), required for the synthesis of the β4TA chelating system, was successfully prepared from Boc-Dap-OH as described in literature.[39] A customized procedure to remove the sulfonamide by-product by buffered extraction was described by Lundquist et al.[40] for the purification of α-azido acids, and was successfully applied to the synthesis of Boc-βN_3Ala-OH.

After coupling the simplest alkynoic acid, propynoic acid (**10**), to the solid-supported peptide, yielding compound **12**, Cu^I-catalyzed cycloaddition was carried out successfully overnight with Boc-βN_3Ala-OH (**16**; 2.0 equiv), DIEA (2.0 equiv), and CuI (0.2 equiv) in DMF. Cleavage of peptide **14** from the resin yielded peptide **4a**. However, the bombesin analogue containing the β4TA chelator **4a** could only be labeled with the $^{99m}Tc(CO)_3$ core in ~60% yield. Moreover, the $^{99m}Tc(CO)_3$ complex of **4a** appeared to be unstable, likely because of the lower electron density at the coordinating N_2 of the triazole ring, which is enhanced by the fact that the carbonyl group forms a conjugated system with the triazole, rendering the ring even more electron deficient.

To increase the distance between the carbonyl and the triazole ring, 4-pentynoic acid (**11**) was coupled to the resin bound peptide **9** (Scheme 2). To maintain a similar spacer length, only one βAla residue was incorporated in this analogue. Subsequently, Boc-βN_3Ala-OH (**16**; 2.0 equiv) was "clicked" to resin-bound peptide **13** (1.0 equiv), using catalytic quantities of CuI (0.2 equiv) and DIEA (2.0 equiv) in DMF. Despite our efforts, we were not able to label compound **4b** in a high yield or obtain the stable $^{99m}Tc(CO)_3$ complex.

Because the glycated counterpart **2** of (*N*$^{\alpha}$His)Ac-βAla-βAla-BBS(7–14)-NH_2 (**1**) displayed an improved biodistribution profile,[28] we also prepared the glycated counterpart of β1TA analogue **3**. For this analogue, both chelator conjugation and glycation were carried out by Cu^I-catalyzed alkyne/azide cycloaddition (Scheme 3). Peptide **17**, containing an alkyne, was Fmoc deprotected and then "clicked" to N_3-β-D-glucose$(OAc)_4$ (**18**; 8.0 equiv), in the presence of DIEA (4.0 equiv) and CuI (0.4 equiv), to provide compound **19**. Subsequently, azidoacetic acid was coupled to the peptide, yielding compound **20**, which was then "clicked" to Boc-Pra-OH (**7**). Compound **21** was then cleaved from the resin and acetates on the glucose moiety were removed by aminolysis in aqueous ammonia/methanol to provide bombesin analogue **5** (see Table 1). These "click" examples further illustrate the general potential for the azide/alkyne cycloaddition reaction in bioconjugation applications.[41]

In vitro and in vivo assays

Radiolabeling

The radiolabeling yields for $[^{99m}Tc(CO)_3]$BBS analogues **3** and **5**, which contain the β1TA chelator, were higher than 95%, which is similar to the labeling yield for the (*N*$^{\alpha}$His)Ac chelator.[35] The physicochemical properties of the labeled and unlabeled pep-

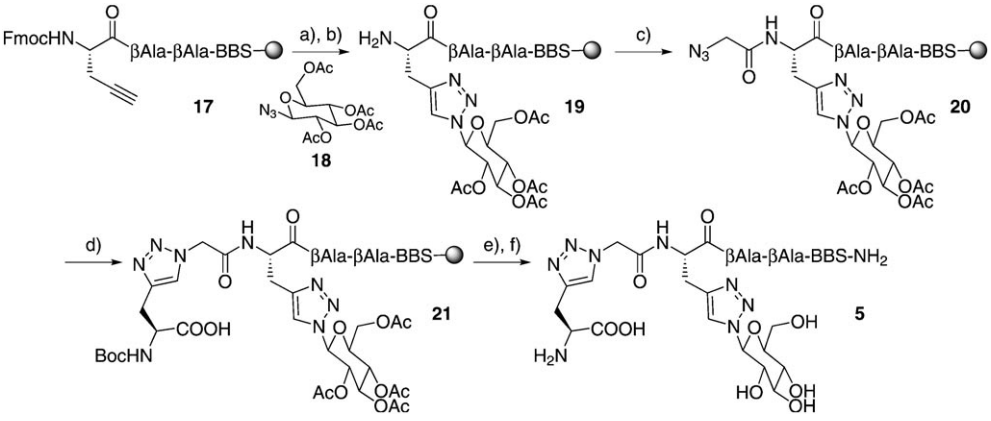

Scheme 3. Synthesis of (β1TA)Ac-Ala(^{N}TG)-βAla-βAla[Cha^{13},Nle^{14}]BBS(7–14): a) 20% piperidine/DMF, 2×10 min; b) N_3-β-D-glucose$(OAc)_4$ (8.0 equiv), CuI (0.4 equiv), DIEA (4.0 equiv), DMF, 16 h; c) N_3CH_2COOH (3.0 equiv), DIC (3.0 equiv), HOBt (3.0 equiv), DMF, 2 h; d) Boc-Pra-OH (2.0 equiv), CuI (0.2 equiv), DIEA (2.0 equiv), DMF, 16 h; e) 10% TA/EDT (7:3) in TFA, 3 h; f) 25% aqueous NH_3/MeOH (1:1), [peptide] = 2 mM, 16 h.

Table 1. Analytical data for bombesin analogues **1**–**5**.

Compd	Formula	Yield [%][a]	$M_{r\,calcd}$ [Da]	ESIMS(+) $[M+H]^+$	HPLC t_R [min]	Purity [%][b]
1	$C_{61}H_{90}N_{18}O_{14}$	47	1298.7	1299.4	13.2	>98
2	$C_{72}H_{106}N_{22}O_{20}$	42	1598.8	1599.4	13.1	>98
3	$C_{57}H_{84}N_{18}O_{13}$	39	1228.6	1229.2	13.4	>98
4a	$C_{59}H_{87}N_{19}O_{14}$	23	1285.7	1286.6	13.4	>98
4b	$C_{58}H_{86}N_{18}O_{13}$	41	1242.7	1243.4	13.4	>98
5	$C_{71}H_{105}N_{23}O_{20}$	30	1599.8	1600.3	12.0	>98

[a] After purification. [b] After preparative HPLC.

tides were sufficiently different to allow simple purification by preparative HPLC. The $[Re(CO)_3]$ complexes of **3** and **5** were prepared, and their identities were confirmed by mass spectrometry. In contrast, the labeling yields of analogues **4a** and **4b**, containing the isomeric β4TA, were lower than 60%. Moreover, these complexes were shown to be unstable (vide infra). The lower labeling yields and stability of $Tc(CO)_3$ complexes involving the β4TA chelator (Scheme 2), compared with those containing the β1TA chelator, have been previously reported (see "inverse click" ligands in reference [30]). This has been attributed to lower electron density at the coordinating N_2 relative to that at the coordinating triazole N_3 in the β1TA chelator.[30] The electron density at N_2 is even lower for **4a**, due to conjugation of the carbonyl group.

Metabolic stability studies

The stability of the new radiolabeled bombesin analogues was determined in human plasma as described in the experimental part, and was in agreement with the stability of our other [Cha[13],Nle[14]]BBS(7–14) peptide analogue.[21] The half-life was determined to be 16 h.

Binding tests

The unlabeled bombesin analogues show high binding affinity for GRP receptors, as shown in Table 2. All of the analogues were able to displace the binding of $^{99m}Tc(CO)_3$-labeled (N^{α}His)Ac-BBS(7–14) to GRP receptors in human prostate adenocarcinoma PC-3 cells, exhibiting IC_{50} values in the nanomolar range. The binding affinity (K_D) of analogues **1**, **2**, **3**, and **5** is in the sub-nanomolar range, indicating that replacement of the (N^{α}His)Ac chelator with the β1TA chelator has no influence on binding affinity. The affinities of radiolabeled compounds **4a** and **4b** could not be determined, likely due to rapid decomposition of the $[^{99m}Tc(CO)_3]$β4TA complex in the in vitro assay conditions used.[30] Therefore, no additional in vitro and in vivo tests were carried out for these compounds. The finding that the labeled analogues exhibited higher binding affinities than their non-labeled counterparts is in agreement with previous observations for bombesin and neurotensin analogues.[21,42,43]

Table 2. Binding to the GRPR in PC-3 cells of the labeled (K_D) and unlabeled (IC_{50}) [Cha[13],Nle[14]]BBS(7–14) analogues.

Compd	IC_{50} [nM]	K_D [nM]
1[a]	5.1±1.7	0.18±0.12
2[b]	3.2±1.2	0.29±0.16
3	1.9±1.1	0.19±0.06
4a	ND	ND[c]
4b	4.2±0.7	ND[c]
5	5.2±0.1	0.60±0.27

[a] Data from Ref. [21], reported here as a reference value. [b] Data from Ref. [27,28], reported here as a reference value. [c] Could not be determined due to instability of the complex.

Internalization and efflux

Based on the internalization and externalization patterns (Figure 2), there are no crucial differences between the analogues. In general, all analogues rapidly internalized, reaching a plateau after 60 min with ~25–35% of the applied dose found inside the cells. From the internalization curves of (N^{α}His)Ac-conjugated bombesin analogues **1** and **2**, it can be concluded that glycation has a positive influence on internalization. The same trend was not observed for β1TA-containing bombesin analogues **3** and **5**. Blockade experiments using an excess of native BBS(1–14) also showed that binding and internalization were very specific. In regard to externalization, no profound differences were observed for analogues **1**, **2**, and **3**; ~30–40% of the internalized activity remained in the cells after 5 h. The β1TA-containing, glycated analogue (**5**) had longer cellular retention than the other analogues, with 60% of the activity remaining in the cells 5 h after maximal internalization.

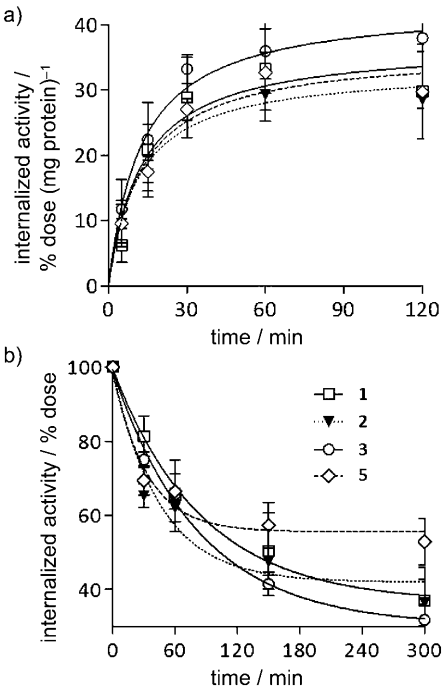

Figure 2. Time course of a) internalization and b) externalization after maximal internalization for $^{99m}Tc(CO)_3$-labeled bombesin analogues **1**, **2**, **3**, and **5** in PC-3 cells after incubation at 37 °C (n = 2–3 in triplicate).

Biodistribution studies

Animal experiments were performed in nude mice bearing PC-3 tumor xenografts with bombesin analogues **3** and **5**. The collected data were compared with reference analogues **1** and **2** (Table 3). At 0.5 h post-injection (p.i.), blood activity was about threefold higher for bombesin analogues **2**, **3**, and **5** than for analogue **1**, although these analogues had a faster rate of clearance. For the unglycated analogues, kidney uptake was higher for analogue **3** at 0.5 h p.i. alone. At later time points, both analogues showed similar renal uptake, due to a faster excretion of compound **3**. For glycated analogues **2** and **5**, uptake in the kidneys was nearly identical for all time points, with a relatively high early uptake followed by fast excretion. Kidney uptake was higher for the glycated analogues than for their unglycated counterparts at all time points, which can be attributed to their higher hydrophilicity and correspondingly lower hepatobiliary excretion. Nevertheless, kidney uptake of all analogues decreased significantly over time, indicating that the radioligand was not trapped in the kidneys.

Table 3. Biodistribution of [^{99m}Tc(CO)$_3$]BBS analogues **1**, **2**, **3**, and **5** in nude mice bearing PC-3 xenografts.[a]

Compd	Organs	0.5 h	1.5 h	5.0 h	1.5 h blocked
1[b]	Blood	0.58 ± 0.21	0.36 ± 0.66	0.23 ± 0.11	0.47 ± 0.07
	Stomach	1.37 ± 0.62	0.73 ± 0.47	0.60 ± 0.33	1.23 ± 0.08
	Kidney	1.82 ± 0.51	0.79 ± 0.35	0.39 ± 0.20	0.76 ± 0.19
	Liver	5.26 ± 1.26	2.36 ± 0.87	1.83 ± 0.75	2.13 ± 0.36
	Small Int	5.00 ± 0.69	1.83 ± 0.57	0.32 ± 0.19	6.48 ± 2.88
	Pancreas	19.00 ± 7.60	6.16 ± 1.80	0.69 ± 0.53	1.19 ± 0.07
	Colon	2.65 ± 0.30	4.36 ± 3.60	2.55 ± 1.77	1.11 ± 0.17
	Tumor	1.53 ± 0.26	0.80 ± 0.35	0.41 ± 0.27	0.37 ± 0.09
3	Blood	1.54 ± 0.30	0.18 ± 0.01	0.06 ± 0.01	0.19 ± 0.08
	Stomach	2.11 ± 0.50	0.92 ± 0.26	0.36 ± 0.01	0.28 ± 0.10
	Kidney	4.86 ± 1.10	1.00 ± 0.11	0.35 ± 0.07	0.84 ± 0.40
	Liver	4.05 ± 0.81	1.15 ± 0.17	0.38 ± 0.06	1.59 ± 0.31
	Small Int	10.05 ± 3.90	7.29 ± 1.99	7.41 ± 3.04	0.87 ± 0.13
	Pancreas	29.52 ± 6.82	12.46 ± 2.91	4.20 ± 0.28	0.80 ± 0.27
	Colon	6.99 ± 1.92	2.67 ± 1.01	3.27 ± 1.25	0.40 ± 0.15
	Tumor	3.76 ± 1.47	1.20 ± 0.75	0.80 ± 0.44	1.02 ± 0.44
2[c]	Blood	1.77 ± 0.16	0.34 ± 0.11	0.07 ± 0.01	0.49 ± 0.15
	Stomach	4.18 ± 0.20	1.82 ± 0.33	0.54 ± 0.12	0.47 ± 0.11
	Kidney	7.48 ± 0.53	2.65 ± 0.80	0.95 ± 0.05	2.06 ± 0.71
	Liver	1.74 ± 0.07	0.64 ± 0.33	0.22 ± 0.01	0.98 ± 0.80
	Small Int	8.51 ± 1.49	4.55 ± 1.24	1.77 ± 0.46	3.64 ± 1.15
	Pancreas	63.17 ± 8.23	26.96 ± 2.53	3.70 ± 1.15	3.33 ± 0.28
	Colon	12.93 ± 1.88	7.31 ± 1.22	6.43 ± 0.79	0.74 ± 0.07
	Tumor	5.64 ± 2.06	3.62 ± 1.09	2.49 ± 1.32	1.01 ± 0.09
5	Blood	1.40 ± 0.39	0.19 ± 0.06	0.08 ± 0.01	0.16 ± 0.03
	Stomach	4.67 ± 2.06	1.46 ± 0.21	0.96 ± 0.33	0.04 ± 0.96
	Kidney	6.36 ± 0.81	2.20 ± 0.60	0.89 ± 0.15	1.63 ± 0.20
	Liver	0.96 ± 0.09	0.31 ± 0.05	0.23 ± 0.07	0.77 ± 0.08
	Small Int	7.21 ± 2.47	3.34 ± 0.61	0.66 ± 0.14	1.32 ± 0.32
	Pancreas	51.99 ± 5.52	31.40 ± 2.81	17.65 ± 2.00	1.91 ± 0.25
	Colon	9.21 ± 2.07	6.14 ± 0.78	4.65 ± 1.75	0.36 ± 0.14
	Tumor	4.97 ± 1.14	4.41 ± 0.55	2.61 ± 0.81	0.68 ± 0.22

[a] Dose: 3.7 MBq per mouse i.v.; animals in the blocked study received an i.v. co-injection of 0.1 mg native BBS(1–14). Data are expressed as a percentage of injected dose per gram of tissue ± SD; $n = 3$–4. [b] Data from Ref. [21]. [c] Data from Ref. [28].

Liver uptake was similar for analogues **1** and **3** at 0.5 h p.i., although analogue **3** had a slightly faster clearance rate. Liver uptake for the glycated analogues was also very similar and was very low at all time points. When the liver uptake for **2** and **5** is compared with unglycated analogues **1** and **3**, it is evident that glycation results in a significant decrease in liver accumulation. The increase in hydrophilicity after glycation decreases hepatobiliary excretion, which explains the observed decrease in liver uptake.

Colon uptake and, more notably, pancreatic uptake, were significant for all analogues. This was expected, as these organs are known to be GRPR-positive in rodents.[4] Uptake in both organs was successfully blocked by co-injection with BBS(1–14) at 1.5 h p.i., demonstrating the high specificity of in vivo uptake. Glycated analogues **2** and **5** were characterized by higher uptake in receptor-positive organs. The presence of the β1TA-containing chelator resulted in slower clearance.

Tumor uptake was similar for compounds **2** and **5**, but higher than for compounds **1** and **3** at all time points. The β1TA glycated analogue (**3**) exhibited a higher tumor uptake than compound **1**, particularly at the earliest p.i. time point. This would indicate that carbohydration has a greater impact on tumor uptake than chelation.

Tumor-to-tissue ratios

Tumor-to-blood ratios indicate the overall radioactive background due to circulation of the radiolabeled compound in the blood, and are a valuable tool to compare the applicability of various radiopharmaceuticals in tumor diagnosis. The tumor-to-blood ratio for analogue **1** remained low at all p.i. time points. In comparison, there was a remarkable increase in the tumor-to-blood ratio for β1TA-containing bombesin counterpart **3** during the same time. Glycated bombesins **2** and **5** had similar tumor-to-blood ratios, except at 1.5 h p.i., and exhibited higher tumor-to-blood ratios relative to the unglycated bombesins. This difference can be explained by the faster blood clearance and higher tumor uptake resulting from glycation (Figure 3).

Tumor-to-kidney ratios were generally lower than the other ratios, due to the constant clearance of radiopharmaceuticals through the renal pathway. Because of the higher tumor uptake for analogues **2**, **3**, and **5** relative to bombesin **1**, the tumor-to-kidney values for the former are higher (Tu/Ki ≈ 2 or 3) than the latter (Tu/Ki ≈ 1) at 5.0 h p.i. (Figure 3).

High tumor-to-liver ratios are preferable, as high uptake in the liver may hamper imaging of abdominal lesions and metastases. For compounds **1** and **3**, tumor-to-liver ratios were fairly low and similar (~1) at early time points, with a small increase for compound **3** observed at 5.0 h p.i. The ratios for **2** and **5** were markedly higher at all time points than those for unglycated analogues **1** and **3**, and increased with time, likely the result of increased hydrophilicity. This higher hydrophilicity after glycation resulted in decreased hepatobiliary excretion and, in turn, lower liver uptake and higher tumor uptake (Figure 3).

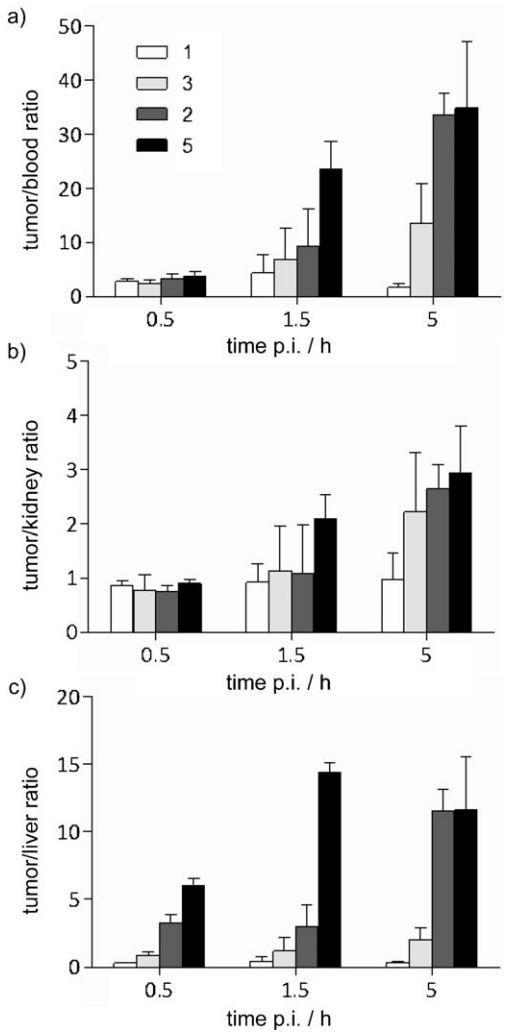

Figure 3. a) Tumor-to-blood, b) tumor-to-kidney, and c) tumor-to-liver ratios at various p.i. time points for glycated and unglycated $^{99m}Tc(CO)_3$-labeled bombesin analogues **1**, **2**, **3**, and **5** in nude mice bearing PC-3 xenografts.

SPECT/CT images were acquired for compounds **1** (unglycated, N^{α}His chelator), **2** (glycated, N^{α}His chelator), and **5** (glycated, βT1A chelator) at 1.5 h p.i. The tumor xenografts were clearly delineated for glycated analogues **2** and **5**, (Figure 4b and 4c), which all showed much lower accumulation in the liver and gastrointestinal tract, due to their higher hydrophilicity and decreased hepatobiliary excretion. In contrast, compound **1** exhibited higher uptake in the abdominal area and lower tumor uptake (Figure 4a), as observed in the biodistribution study. Similar imaging results were obtained for both glycated analogues, indicating that the chelator has no influence on pharmacokinetic properties.

Conclusions

The β-[1-(peptidyl)-1*H*-1,2,3-triazol-4-yl]Ala chelator, termed β1TA, can be easily conjugated to a solid-supported peptide sequence before labeling in high yield with the $^{99m}Tc(CO)_3$ core. Compared with the (N^{α}His)Ac chelator, the β1TA chelator has a major advantage in that it does not contain a reactive secondary amine, which may cause a selectivity problem during the conjugation of other molecules to the peptide, such as carbohydrates or fluorophores. In contrast, the second type of triazole chelator, the β-[4-(peptidyl)-1*H*-1,2,3-triazol-1-yl]Ala, or β4TA, chelator,β4TA although equally straightforward to synthesize, did not form stable complexes with the $^{99m}Tc(CO)_3$ core and is therefore not suitable for radiolabeling.

No notable differences were observed in the in vitro properties of the studied analogues, except for the slightly lower externalization of compound **5** despite a lower internalization. With regard to biodistribution, only a few differences were found for the β1TA-containing compounds relative to their (N^{α}His)Ac-conjugated counterparts. More remarkable differences were observed after glycation, with both the β1TA-containing glycated analogue (**5**) and the (N^{α}His)Ac glycated analogue (**2**) exhibiting better biodistribution, with higher tumor uptake and lower liver uptake, as a result of the shift from hepatobili-

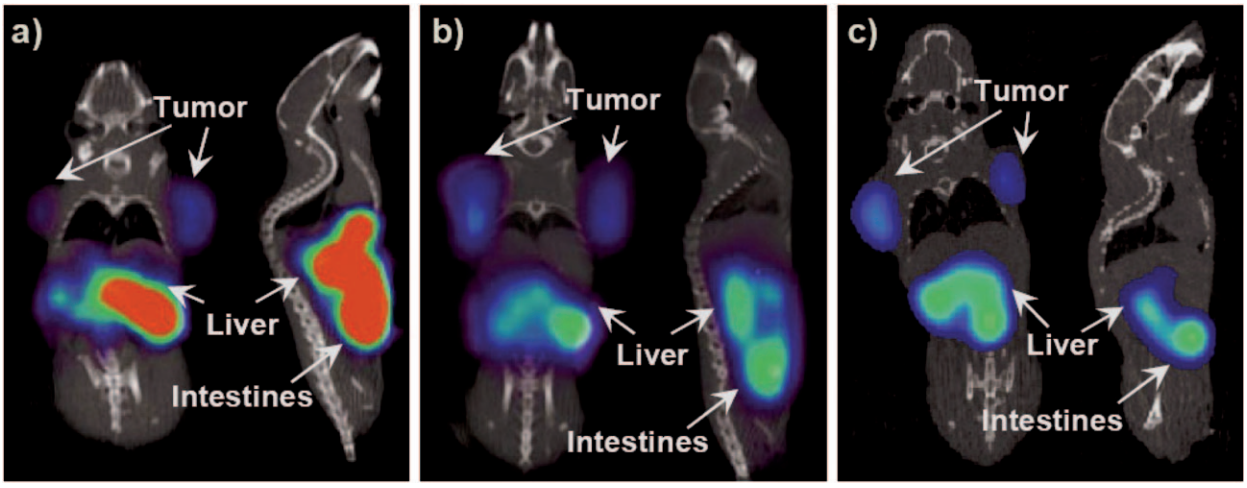

Figure 4. SPECT/CT imaging of nude mice with PC-3 tumor xenografts 1.5 h after injection of the radiolabeled BBS analogues (20 MBq, i.v.). The images correspond to the coronal (left) and sagittal (right) sections for a) compound **1**, b) compound **2**, and c) compound **5**.

ary to renal excretion. This led to bombesin analogues with greater potential for future targeting of bombesin receptor-positive tumors.

Experimental Section

The Supporting Information contains information on chemical suppliers and equipment, an overview of methods used for compound analysis and purification, and HPLC and MS data for the prepared BBS analogues. Azidoacetic acid and trifluoromethanesulfonyl azide were prepared as described.[40,44] Reference peptides **1** and **2** were prepared as previously described by our research group.[21,27]

General protocol for peptide synthesis and purification

The peptide analogues were synthesized manually in plastic syringes (2.5–5 mL) with a PE frit (MultiSynTech GmbH, Germany) on Rink amide polystyrene resin, according to the Fmoc peptide synthesis protocol. The resin (0.60 mmol g^{-1}) was weighed and swollen in CH_2Cl_2 for 10 min. The solvent was removed by filtration, and the resin was washed with DMF. The entire peptide sequence was synthesized by consecutive Fmoc deprotections and amino acid couplings. After each Fmoc deprotection and coupling step, solvent and reagents were removed by filtration and by thorough washing of the resin with DMF, *i*PrOH, and then DMF again. Fmoc deprotections were carried out in a 20% solution of piperidine/DMF (2× 10 min). Each amino acid coupling was performed by adding the Fmoc protected amino acid (3.0 equiv), with DIC (3.0 equiv) and HOBt (3.0 equiv), to the resin in DMF ([Fmoc-AA-OH] ≈ 0.5 M). The mixture was allowed to shake for 2 h. Coupling of Fmoc-Nle-OH to the resin was performed twice. Completeness of the other couplings was assessed by the ninhydrin test, and coupling was only repeated for those reactions with positive test results.[45]

Peptides were cleaved from the Rink amide resin by the addition of a TFA/thioanisole/ethanedithiol (90:7:3) mixture to the resin in the plastic syringe (~0.3 mL per 100 mg resin). The mixture was allowed to shake for 3 h at 25 °C before the resin was filtered. The filtrate was collected in a Falcon tube containing 10 mL cold Et_2O, which caused the peptide to precipitate. The tube was stored at 4 °C for 30 min, then the peptide was isolated by centrifugation and decanting of the Et_2O. Et_2O was again added to the peptide in the tube and the centrifugation and decantation processes were repeated twice more. The crude peptide was then purified by preparative HPLC.

Synthesis of Boc-βN$_3$Ala-OH (17). TfN_3 (2.0 equiv) was added dropwise to a solution of 213 mg Boc-Dap-OH (1.0 equiv), 216 mg K_2CO_3 (1.5 equiv), and 2.6 mg $CuSO_4 \cdot 5H_2O$ (0.01 equiv) in 20 mL H_2O/MeOH (1:2). The reaction mixture stirred for 16 h, then the organic solvents were removed in vacuo and the remaining aqueous solution was diluted with 50 mL H_2O. The solution was acidified with 37% $HCl_{(aq)}$ to pH 6. Next, 50 mL of 0.25 M phosphate buffer (pH 6.2, 6.8 g KH_2PO_4 and 0.88 g K_2HPO_4 in 200 mL H_2O) were added and the aqueous phase was extracted with EtOAc (4× 15 mL). The aqueous phase was acidified to pH 2 with 37% $HCl_{(aq)}$ and extracted with CH_2Cl_2 (4×50 mL). The combined CH_2Cl_2 phases were dried over $MgSO_4$, filtered, and concentrated under reduced pressure to obtain a colorless oil in 61% yield (147 mg). $R_f = 0.1$ (EtOAc); ^{1}H NMR (250 MHz, $CDCl_3$): $\delta = 1.47$ (s, 9H), 3.58–3.99 (m, 2H), 4.50–4.65 (m, 1H), 5.45 (d, $^3J_{HH} = 7.1$ Hz, 1H); ^{13}C NMR (63 MHz, $CDCl_3$): $\delta = 28.2$, 52.4, 53.3, 81.0, 155.4, 173.9; MS (ESI+) *m/z* $[M+H]^+$: 231.

Synthesis of β1TA-CH$_2$CO-βAla-[Cha^{13},Nle^{14}]BBS(7–14)-NH$_2$ (3). The solid-supported βAlaGln(Trt)Trp(Boc)AlaValGlyHis(Trt)ChaNle peptide sequence was synthesized as described in the solid-phase peptide synthesis section. Azidoacetic acid (3.0 equiv)[44] was subsequently coupled to this peptide using DIC (3.0 equiv) and HOBt (3.0 equiv) in DMF. After 2.0 h, the solvent and reagents were removed by filtration, and the resin was washed with DMF, *i*PrOH, and then DMF again. A solution of Boc-Pra-OH (2.0 equiv), CuI (0.2 equiv), and DIEA (2.0 equiv) in DMF was added to the resin, and the reaction mixture was allowed to shake for 16 h at 25 °C. The solvent and reagents were removed by filtration, and the resin was washed with DMF, *i*PrOH and Et_2O and dried under reduced pressure. Finally, peptide **3** was obtained following resin cleavage and purification as described in the general procedure above.

Synthesis of β4TA-CO-βAla-βAla-[Cha^{13},Nle^{14}]BBS(7–14)-NH$_2$ (4a). The solid-supported βAlaβAlaGln(Trt)Trp(Boc)AlaValGlyHis(Trt)ChaNle peptide sequence was synthesized as described in the solid-phase peptide synthesis section. Propynoic acid (3.0 equiv) was subsequently coupled to this peptide using DIC (3.0 equiv) and HOBt (3.0 equiv) in DMF. After 2.0 h, the solvent and reagents were removed by filtration, and the resin was washed with DMF, *i*PrOH, and then DMF again. Next, Boc-βN$_3$Ala-OH (2.0 equiv), CuI (0.2 equiv), and DIEA (2.0 equiv) in DMF were added to the resin. The reaction mixture was allowed to shake for 16 h at 25 °C. The solvent and reagents were removed by filtration, and the resin was washed with DMF, *i*PrOH and Et_2O and dried under reduced pressure. Peptide **4a** was obtained following resin cleavage and purification as described in the general procedure above.

Synthesis of β4TA-CH$_2$CH$_2$CO-βAla-[Cha^{13},Nle^{14}]BBS(7–14)-NH$_2$ (4b). The synthesis of compound **4b** differed only in the spacer from the preparation of compound **4a**. The spacer of compound **4b** contains a pentynoic acid and only one βAla residue.

Synthesis of β1TA-CH$_2$CO-Ala(^{N}TG)-βAla-βAla-[Cha^{13},Nle^{14}]BBS(7–14)-NH$_2$ (5). The solid-supported PraβAlaβAlaGln(Trt)Trp(Boc)AlaValGlyHis(Trt)ChaNle peptide sequence was synthesized as described in the solid-phase peptide synthesis section. Next, N$_3$-β-D-glucose(OAc)$_4$ (8.0 equiv), CuI (0.4 equiv), and DIEA (4.0 equiv) in DMF were added to the resin. The reaction mixture was allowed to shake for 16 h at 25 °C, then the solvent and reagents were removed by filtration, and the resin was washed with DMF, *i*PrOH, and then DMF again. Azidoacetic acid (3.0 equiv) was subsequently coupled to the peptide using DIC (3.0 equiv) and HOBt (3.0 equiv) in DMF. After 2.0 h, the solvent and reagents were removed by filtration, and the resin was washed with DMF, *i*PrOH, and then DMF again. Then a solution of Boc-Pra-OH (2.0 equiv), CuI (0.2 equiv), and DIEA (2.0 equiv) in DMF were added to the resin. The reaction mixture was allowed to shake for 16 h at 25 °C. The solvent and reagents were removed by filtration, and the resin was washed with DMF, *i*PrOH, and Et_2O and dried under reduced pressure. After simultaneous deprotection of functional groups and cleavage of the peptide from the resin, as described in the general procedure above, the crude peptide was dissolved in a 25% aqueous NH_3 (pH 9)/MeOH (1:1) solution and stirred for 24 h at 25 °C. The crude reaction mixture was purified by preparative HPLC.

Labeling procedures

^{99m}Tc(CO)$_3$ labeling

Approximately 1 mL of a Na[^{99m}TcO$_4$] (~5 GBq) was eluted from a generator and was added to the Isolink mixture, containing Na_2-(H_3BCO_2) (4.5 mg), borax (2.9 mg), K-Na tartrate tetrahydrate

(9 mg), and Na_2CO_3 (7–8 mg). This mixture was heated for 20 min at 100 °C and subsequently adjusted to pH 6.5 with a mixture of HCl and phosphate buffer; 500 μL were withdrawn and combined with 15–30 μL of the peptide solution (1 mM), following by heating of the mixture at 75 °C for 1 h to enable labeling.

$Re(CO)_3$ labeling

$[ReBr_3(CO)_3][Et_4N]_2$ (10^{-3} M in H_2O, 200 μL) was added to a solution of bombesin analogue **3** or **5** in H_2O (10^{-3} M, 100 μL), and the solution was heated at 100 °C for 1 h. HPLC analysis indicated complete conversion of the starting material. The complexes were characterized by ESIMS: $[Re(CO)_3(\mathbf{3})]$: $C_{60}H_{83}N_{18}O_{16}Re$; calcd m/z $[M+H]^+ = 1499.6$; $[M+2H]^+/2 = 750.3$, found 1499.7 and 750.3. $[Re(CO)_3(\mathbf{5})]$: $C_{74}H_{103}N_{23}O_{23}Re$; calcd m/z $[M+H]^+ = 1868.7$; $[M+H]^+/2 = 935.9$, found 935.9.

In vitro biological evaluation of peptides

Cell line

Cells were maintained in DMEM with GLUTAMAX-I, supplemented with 10% FCS, 100 IU mL^{-1} penicillin G sodium, 100 μg mL^{-1} streptomycin sulfate, and 0.25 μg mL^{-1} amphotericin B. They were incubated at 37 °C in an atmosphere containing 5% CO_2 and were subcultured twice weekly after detaching the cells with trypsin-EDTA.

Metabolic stability studies

The metabolic stability of the radiolabeled analogues was determined in human plasma. Each analogue (3–4 MBq mL^{-1}, 1.5–2 pmol mL^{-1}) was incubated for different time periods (from 0–24 h) at 37 °C. Following incubation, proteins were precipitated with CH_3CN/EtOH (1:1) and TFA (0.01%) and were centrifuged at 4 °C (10 min, 20000 g). The supernatant was filtered and analyzed by RP-HPLC. Different peaks corresponding to the intact peptide and the degradation products were observed in the radioactivity chromatograms. The percentage of intact peptide was determined for each incubation time.

Binding assays

Inhibition studies

Intact human prostate adenocarcinoma PC-3 cells at confluence were placed in 48-well plates. After 24 h, the cells were incubated with increasing concentrations of BBS analogues (0–30000 nM), in the presence of 4 kBq of $^{99m}Tc(CO)_3$-(N^{α}His)Ac-BBS(7–14) for 1 h at 37 °C. A specific binding buffer was used that includes protease inhibitors (50 mM HEPES, 125 mM NaCl, 7.5 mM KCl, 5.5 mM $MgCl{\cdot}6H_2O$, 1 mM EGTA, 5 g L^{-1} BSA, 2 mg L^{-1} chymostatin, 100 mg L^{-1} soybean trypsin inhibitor, 50 mg L^{-1} bacitracin, pH 7.4). Next, the cells were washed twice with cold PBS. Bound radioactivity was recovered by solubilizing the cells in 1 N NaOH (2×400 μL) at 37 °C, with radioactivity measured in a γ counter. Experiments were performed 2–3 times in triplicate.

Saturation studies

Cells were placed in 48-well plates and, after 24 h, were incubated with increasing concentrations of the labeled BBS analogues (0.01–2 nM) for 1 h at 37 °C in the binding buffer described above. Non-specific binding was determined by co-incubation with 1 μM natural BBS. After 1 h, the cells were washed twice with cold PBS and solubilized in 1 N NaOH (2×400 μL). Radioactivity was measured by γ counter, and experiments were performed 2–3 times in triplicate.

Internalization

PC-3 cells at confluence were placed in 6-well plates. 24 h later, they were incubated with labeled analogues (2–4 kBq) in culture medium for 5, 15, 30, 60 and 120 min at 37 °C. To determine non-specific binding, 1 μM natural BBS was added. After incubation, the supernatant was collected and the cells were washed twice with cold PBS. Surface-bound activity was removed by acid wash (50 mM glycine/HCl, 100 mM NaCl, pH 2.8, 2×600 μL for 5 min) and collected. Internalized activity was measured by lysing the cells with 1 N NaOH (2×600 μL). Radioactivity of all collected fractions was measured by γ counter. Results are expressed as percentage of total added radioactivity per mg protein. Experiments were performed 2–3 times in triplicate.

Efflux

For externalization studies, PC-3 cells at confluence were incubated with labeled analogues (2–4 kBq well^{-1}) in culture medium for 1 h at 37 °C to allow binding and maximal internalization. The supernatant was discarded, and the cells were washed twice with cold PBS. New medium (2 mL) was added, and the cells were incubated again at 37 °C for various times (30, 60, 150 and 300 min). The supernatant was collected, and the cells were washed twice with cold PBS. Internalized radioactivity was measured by lysing the cells with 1 N NaOH (2×600 μL). Radioactivity of the supernatant (externalized activity) and of the lysate (internalized activity) was determined by γ counter. Results are expressed as a percentage of the total activity associated with the cells. Experiments were performed 2–3 times in triplicate.

In vivo biological evaluation of peptides

Biodistribution

All animal experiments were conducted in compliance with the Swiss animal protection laws and with the ethical principles and guidelines for scientific animal trials established by the Swiss Academy of Medical Sciences and the Swiss Academy of Natural Sciences. Female CD-1 *nu/nu* mice 6–8 weeks old (Charles River Laboratories, Sulzfeld, Germany) were subcutaneously injected with 8×10^6 PC-3 cells in 150 μL culture medium without supplements. Approximately three weeks after tumor implantation, the mice (3–6 per group) were injected i.v. with 3–4 MBq of the radiolabeled peptide (0.2 pmol per mouse). At 0.5, 1.5, and 5 h p.i., the animals were sacrificed by cervical dislocation. The organs (heart, lung, spleen, kidneys, pancreas, stomach, small intestine, large intestine, liver, muscle, bone), tumor xenografts, and blood were collected and weighed, and the radioactivity was measured by γ counter. To determine the specificity of in vivo uptake, one group of mice received a co-injection of 100 μg unlabeled natural BBS(1–14) and the radiolabeled analogue and were sacrificed 1.5 h p.i. Results are expressed as a percentage of injected dose per gram of tissue.

Imaging

Single-photon emission computed tomography/X-ray computed tomography (SPECT/CT) images were collected postmortem, 1.5 h after i.v. injection of the $^{99m}Tc(CO)_3$-labeled BBS (20 MBq). Images were obtained on a X-SPECT system (Gamma Medica, Inc.), equipped with a single head SPECT device and a CT device. SPECT

data were acquired and reconstructed with LumaGEM (version 5.407). CT data were acquired by an X-Ray CT system (Gamma Medica) and reconstructed with Cobra software (version 4.5.1). Fusion of SPECT and CT data was performed with IDL Virtual Machine (version 6.0). Images were generated with Amira (version 4.0).

List of abbreviations

(*N*$^{\alpha}$His)Ac*N*$^{\alpha}$-carboxymethylhistidine
β1TA β-[1-(peptidyl)-1*H*-1,2,3-triazol-4-yl]Ala
β4TA β-[4-(peptidyl)-1*H*-1,2,3-triazol-1-yl]Ala
BBS bombesin
Boc *tert*-butyloxycarbonyl
Cha cyclohexylalanine
Dap 2,3-diaminopropionic acid
DIC diisopropylcarbodiimide
DIEA *N*,*N*-diisopropylethylamine
DMF dimethylformamide
EDT ethanedithiol
Fmoc 9-fluorenylmethyloxycarbonyl
GRP gastrin-releasing peptide
HOBt 1-hydroxybenzotriazole
Nle norleucine
NMB neuromedin B
PC-3 human prostate adenocarcinoma cell line
Pra propargylglycine
TA thioanisole
TFA trifluoroacetic acid
TfN_3 trifluoromethanesulfonyl azide

Acknowledgements

L.B. thanks the Institute for the Promotion of Innovation through Science and Technology in Flanders (IWT-Vlaanderen) for grant support. V.M. is a postdoctoral researcher for the Fund for Scientific Research (Flanders). This work was funded by FWO grant G.0036.04 and by Swiss Cancer League grant KLS 02040-02-2007.

Keywords: bombesin · chelators · click chemistry · radiochemistry · triazolyl · tumor targeting

[1] A. Anastasi, V. Erspamer, M. Bucci, *Experientia* **1971**, *27*, 166 – 167.
[2] T. J. McDonald, H. Jörnvall, G. Nilsson, M. Vagne, M. Ghatei, S. R. Bloom, V. Mutt, *Biochem. Biophys. Res. Commun.* **1979**, *90*, 227 – 233.
[3] N. Minamino, T. Sudoh, K. Kangawa, H. Matsuo, *Biochem. Biophys. Res. Commun.* **1985**, *130*, 685 – 691.
[4] R. T. Jensen, J. F. Battey, E. R. Spindel, R. V. Benya, *Pharmacol. Rev.* **2008**, *60*, 1 – 42.
[5] D. C. Heimbrook, M. E. Boyer, V. M. Garsky, N. L. Balishin, D. M. Kiefer, A. Oliff, M. W. Riemen, *J. Biol. Chem.* **1988**, *263*, 7016 – 7019.
[6] W. Marki, M. Brown, J. E. Rivier, *Peptides* **1981**, *2*, 169 – 177.
[7] C. J. Smith, W. A. Volkert, T. J. Hoffman, *Nucl. Med. Biol.* **2003**, *30*, 861 – 868.
[8] F. Cuttitta, D. N. Carney, J. Mulshine, T. W. Moody, J. Fedorko, A. Fischler, J. D. Minna, *Nature* **1985**, *316*, 823 – 826.
[9] M. Gugger, J. C. Reubi, *Am. J. Pathol.* **1999**, *155*, 2067 – 2076.
[10] R. Markwalder, J. C. Reubi, *Cancer Res.* **1999**, *59*, 1152 – 1159.
[11] J. J. Parry, R. Andrews, B. E. Rogers, *Breast Cancer Res. Treat.* **2007**, *101*, 175 – 183.
[12] S. S. Radulovic, S. R. Milovanovic, R. Z. Cai, A. V. Schally, *Proc. Soc. Exp. Biol. Med.* **1992**, *200*, 394 – 401.
[13] J. Y. Shi, B. Jia, Z. F. Liu, Z. Yang, Z. L. Yu, K. Chen, X. Y. Chen, S. Liu, F. Wang, *Bioconjugate Chem.* **2008**, *19*, 1170 – 1178.
[14] J. H. Zhou, J. Chen, M. Mokotoff, R. K. Zhong, L. D. Shultz, E. D. Ball, *Clin. Cancer Res.* **2003**, *9*, 4953 – 4960.
[15] J. C. Reubi, *Endocr. Rev.* **2003**, *24*, 389 – 427.
[16] I. U. Khan, A. G. Beck-Sickinger, *Anti-Cancer Agents Med. Chem.* **2008**, *8*, 186 – 199.
[17] B. Nock, A. Nikolopoulou, A. Galanis, P. Cordopatis, B. Waser, J. C. Reubi, T. Maina, *J. Med. Chem.* **2005**, *48*, 100 – 110.
[18] J. Schuhmacher, H. W. Zhang, J. Doll, H. R. Mäcke, R. Matys, H. Hauser, M. Henze, U. Haberkorn, M. Eisenhut, *J. Nucl. Med.* **2005**, *46*, 691 – 699.
[19] H. Zhang, J. Chen, C. Waldherr, K. Hinni, B. Waser, J. C. Reubi, H. R. Maecke, *Cancer Res.* **2004**, *64*, 6707 – 6715.
[20] X. Z. Zhang, W. B. Cai, F. Cao, E. Schreibmann, Y. Wu, J. C. Wu, L. Xing, X. Y. Chen, *J. Nucl. Med.* **2006**, *47*, 492 – 501.
[21] E. García-Garayoa, D. Rüegg, P. Bläuenstein, M. Zwimpfer, I. U. Khan, V. Maes, A. Blanc, A. G. Beck-Sickinger, D. A. Tourwé, P. A. Schubiger, *Nucl. Med. Biol.* **2007**, *34*, 17 – 28.
[22] C. J. Smith, H. Gali, G. L. Sieckman, C. Higginbotham, W. A. Volkert, T. J. Hoffman, *Bioconjugate Chem.* **2003**, *14*, 93 – 102.
[23] H. J. Wester, M. Schottelius, K. Scheidhauer, J. C. Reubi, I. Wolf, M. Schwaiger, *Eur. J. Nucl. Med. Mol. Imaging* **2002**, *29*, 28 – 38.
[24] T. J. Hoffman, H. Gali, C. J. Smith, G. L. Sieckman, D. L. Hayes, N. K. Owen, W. A. Volkert, *J. Nucl. Med.* **2003**, *44*, 823 – 831.
[25] J. J. Parry, T. S. Kelly, R. Andrews, B. E. Rogers, *Bioconjugate Chem.* **2007**, *18*, 1110 – 1117.
[26] C. J. Smith, G. L. Sieckman, N. K. Owen, D. L. Hayes, D. G. Mazuru, R. Kannan, W. A. Volkert, T. J. Hoffman, *Cancer Res.* **2003**, *63*, 4082 – 4088.
[27] L. Brans, V. Maes, E. García-Garayoa, C. Schweinsberg, S. Däpp, P. Bläuenstein, P. A. Schubiger, R. Schibli, D. A. Tourwé, *Chem. Biol. Drug Des.* **2008**, *72*, 496 – 506.
[28] C. Schweinsberg, V. Maes, L. Brans, P. Bläuenstein, D. A. Tourwé, P. A. Schubiger, R. Schibli, E. García-Garayoa, *Bioconjugate Chem.* **2008**, *19*, 2432 – 2439.
[29] V. Maes, D. Tourwé, *Int. J. Pept. Res. Ther.* **2006**, *12*, 197 – 202.
[30] T. L. Mindt, H. Struthers, L. Brans, T. Anguelov, C. Schweinsberg, V. Maes, D. Tourwé, R. Schibli, *J. Am. Chem. Soc.* **2006**, *128*, 15096 – 15097.
[31] T. L. Mindt, C. Schweinsberg, L. Brans, A. Hagenbach, U. Abram, D. Tourwé, E. García-Garayoa, R. Schibli, *ChemMedChem* **2009**, *4*, 529 – 539.
[32] C. W. Tornøe, C. Christensen, M. Meldal, *J. Org. Chem.* **2002**, *67*, 3057 – 3064.
[33] H. C. Kolb, M. G. Finn, K. B. Sharpless, *Angew. Chem.* **2001**, *113*, 2056 – 2075, *Angew. Chem. Int. Ed.* **2001**, *40*, 2004 – 2021.
[34] H. C. Kolb, K. B. Sharpless, *Drug Discovery Today* **2003**, *8*, 1128 – 1137.
[35] A. Egli, R. Alberto, L. Tannahill, R. Schibli, U. Abram, A. Schaffland, R. Waibel, D. Tourwé, L. Jeannin, K. Iterbeke, P. A. Schubiger, *J. Nucl. Med.* **1999**, *40*, 1913 – 1917.
[36] J. K. Pak, P. Benny, B. Spingler, K. Ortner, R. Alberto, *Chem. Eur. J.* **2003**, *9*, 2053 – 2061.
[37] D. S. Moore, S. D. Robinson, *Adv. Inorg. Chem.* **1988**, *32*, 171 – 239.
[38] E. García-Garayoa, C. Schweinsberg, V. Maes, D. Rüegg, A. Blanc, P. Bläuenstein, D. A. Tourwé, A. G. Beck-Sickinger, P. A. Schubiger, *Q. J. Nucl. Med. Mol. Imaging* **2007**, *51*, 42 – 50.
[39] P. B. Alper, S. C. Hung, C. H. Wong, *Tetrahedron Lett.* **1996**, *37*, 6029 – 6032.
[40] J. T. Lundquist, J. C. Pelletier, *Org. Lett.* **2001**, *3*, 781 – 783.
[41] K. Nwe, M. W. Brechbiel, *Cancer Biother. Radiopharm.* **2009**, *24*, 289 – 302.
[42] M. Bruehlmeier, E. García-Garayoa, A. Blanc, B. Holzer, S. Gergely, D. Tourwé, P. A. Schubiger, P. Bläuenstein, *Nucl. Med. Biol.* **2002**, *29*, 321 – 327.
[43] E. García-Garayoa, P. Bläuenstein, M. Bruehlmeier, A. Blanc, K. Iterbeke, P. Conrath, D. Tourwé, P. A. Schubiger, *J. Nucl. Med.* **2002**, *43*, 374 – 383.
[44] L. A. Banaszynski, T. J. Wandless, *Chem. Biol.* **2006**, *13*, 11 – 21.
[45] E. Kaiser, R. L. Colescott, C. D. Bossinger, P. I. Cook, *Anal. Biochem.* **1970**, *34*, 595 – 598.

Received: May 2, 2010
Revised: July 20, 2010
Published online on August 30, 2010

